



Journal of Coordination Chemistry

Publication details, including instructions for authors and subscription information:

<http://www.tandfonline.com/loi/gcoo20>

Preparation, characterization, and properties of two rare earth organic frameworks with 1H-benzimidazole-2-carboxylic acid

Chengfang Qiao^{a b}, Zhengqiang Xia^a, Qing Wei^a, Chunsheng Zhou^b, Guochun Zhang^b, Sanping Chen^a & Shengli Gao^{a b}

^a Key Laboratory of Synthetic and Natural Functional Molecule Chemistry of Ministry of Education, College of Chemistry and Materials Science, Northwest University, Xi'an, China

^b Shaanxi Key Laboratory of Comprehensive Utilization of Tailing Resources, Department of Chemistry and Chemical Engineering, Shangluo University, Shangluo, China

Accepted author version posted online: 26 Feb 2013. Published online: 05 Apr 2013.

To cite this article: Chengfang Qiao, Zhengqiang Xia, Qing Wei, Chunsheng Zhou, Guochun Zhang, Sanping Chen & Shengli Gao (2013) Preparation, characterization, and properties of two rare earth organic frameworks with 1H-benzimidazole-2-carboxylic acid, Journal of Coordination Chemistry, 66:7, 1202-1210, DOI: [10.1080/00958972.2013.775574](http://dx.doi.org/10.1080/00958972.2013.775574)

To link to this article: <http://dx.doi.org/10.1080/00958972.2013.775574>

PLEASE SCROLL DOWN FOR ARTICLE

Taylor & Francis makes every effort to ensure the accuracy of all the information (the "Content") contained in the publications on our platform. However, Taylor & Francis, our agents, and our licensors make no representations or warranties whatsoever as to the accuracy, completeness, or suitability for any purpose of the Content. Any opinions and views expressed in this publication are the opinions and views of the authors, and are not the views of or endorsed by Taylor & Francis. The accuracy of the Content should not be relied upon and should be independently verified with primary sources of information. Taylor and Francis shall not be liable for any losses, actions, claims, proceedings, demands, costs, expenses, damages, and other liabilities whatsoever or howsoever caused arising directly or indirectly in connection with, in relation to or arising out of the use of the Content.

This article may be used for research, teaching, and private study purposes. Any substantial or systematic reproduction, redistribution, reselling, loan, sub-licensing, systematic supply, or distribution in any form to anyone is expressly forbidden. Terms & Conditions of access and use can be found at <http://www.tandfonline.com/page/terms-and-conditions>

Preparation, characterization, and properties of two rare earth organic frameworks with 1*H*-benzimidazole-2-carboxylic acid

CHENGFANG QIAO^{†‡}, ZHENGQIANG XIA[†], QING WEI^{*†}, CHUNSHENG ZHOU[‡],
GUOCHUN ZHANG[‡], SANPING CHEN^{*†} and SHENGLI GAO^{†‡}

[†]Key Laboratory of Synthetic and Natural Functional Molecule Chemistry of Ministry of Education, College of Chemistry and Materials Science, Northwest University, Xi'an, China

[‡]Shaanxi Key Laboratory of Comprehensive Utilization of Tailing Resources, Department of Chemistry and Chemical Engineering, Shangluo University, Shangluo, China

(Received 7 October 2012; in final form 10 December 2012)

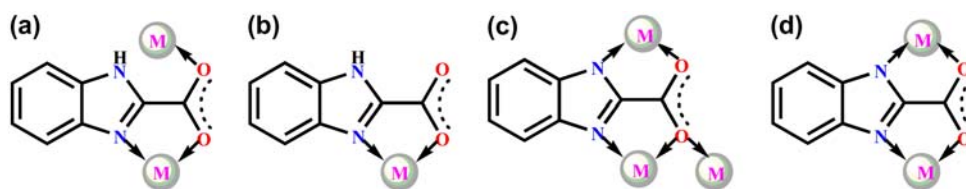
Reaction of rare earth metal ions with 1*H*-benzimidazole-2-carboxylic acid (H₂BIC) acid yielded two rare earth organic frameworks [Ln(HBIC)₃]_n (Ln = Gd **1**, Y **2**; H₂BIC) under hydrothermal conditions. Both compounds were structurally characterized by single-crystal X-ray diffraction. Their thermal stabilities, luminescent, and magnetic properties were also investigated. Compounds **1** and **2** are isomorphic and present 2-D networks constructed by bridging-chelating HBIC[−] linkers and rare earth cation nodes, in which each asymmetric unit consists of one crystallographically unique Ln(III) ion and three HBIC[−] with two kinds of coordination modes. The two compounds exhibit high-thermal stability, stable to 320 °C. Antiferromagnetic interactions between Gd(III) centers for **1** were observed from magnetic susceptibility data. **2** exhibits a strong blue emission band in the solid state.

Keywords: Rare earth organic frameworks; 1*H*-Benzimidazole-2-carboxylic acid; Antiferromagnetic interaction; Luminescence

1. Introduction

Rare earth ions with special chemical/physical characteristics have triggered a wide range of technological applications in optoelectronic devices and magnetic materials [1–6]. Moreover, because of their large radii, high coordination numbers and flexible coordination geometries, rare earth ions are good candidates to construct rare earth organic frameworks with intriguing architectures and potential applications in gas storage, catalysis, ion exchange, and additives in metallurgy [7–10]. It is thus not surprising that such compounds attract interest. Design and assembly of multifunctional rare earth metal-organic frameworks (MOFs) are challenging owing to buried valence orbitals and unspecific coordination properties (variable coordination numbers (6 < CN < 12) and various coordination environments) of rare earth ions [11, 12].

*Corresponding authors. Email: weiqq@126.com (Q. Wei); Sanpingchen@126.com (S. Chen).



Scheme 1. Coordination modes of H_2BIC (M =metal ion).

Structures and performances of MOFs are influenced by many factors, especially the nature of organic linkers, which can act as magnetic mediators and/or luminescent sensitizers [13–17]. Therefore, a well-selected ligand is one of the key factors in the construction of MOFs with desired structures and expected properties. Considering that the rare earth ions have high affinity and prefer to bind to hard donors, rigid multidentate carboxylate-containing ligands may be better choices to prepare rare earth MOFs [18–20].

A multidentate chelating-bridging ligand, 1*H*-benzimidazole-2-carboxylic acid (H_2BIC), evoked our interest for the following reasons: (i) this ligand contains one carboxylic group and two nitrogens from a rigid imidazole ring, so it may coordinate through a number of different coordination fashions (scheme 1). (ii) The delocalized π -electron system of the benzimidazole could be used to stimulate rare earth ion luminescence as an effective chromophore [21, 22]. (iii) The completely or partially deprotonated formations of H_2BIC ligand are beneficial to form hydrogen bonds, generating multidimensional and stable supramolecular architectures. (iv) Some transition metal coordination compounds with H_2BIC have been isolated [23–26]; however, reports on rare earth compounds containing H_2BIC are scarce.

Hydrothermal synthesis has been a powerful technique for the preparation of new materials with diverse structural architectures [27, 28]. Under relatively high temperature and pressure, the problems associated with ligand solubility can be solved, and thus, the reactivity of reactants in crystallization was enhanced.

In this context, hydrothermal reactions of rare earth salts with H_2BIC generated two new 2-D MOFs, $[\text{Ln}(\text{HBIC})_3]_n$ ($\text{Ln}=\text{Gd}$ **1**, Y **2**). Thermal analyzes show that both possess good thermal stability. The magnetism of **1** and luminescence of **2** were also investigated.

2. Experimental

2.1. Materials and analytical methods

H_2BIC was prepared as described [29]. Other chemicals and solvents used were obtained from commercial sources and used as received. Elemental analyzes (C, H, and N) were carried out with an Elementar Vario EL III analyzer. Fourier transform IR spectra were measured on a Tensor 27 spectrometer (Bruker Optics, Ettlingen, Germany) as KBr pellets from 4000 to 400 cm^{-1} . TG and DSC experiments were carried out in air using a NET-ZSCH STA 449F3 equipment at a heating rate of $10^\circ\text{C min}^{-1}$ from 30 to 800°C ; an empty Al_2O_3 crucible was used as reference. Powder X-ray diffraction (PXRD) data were recorded on a Bruker D8 AVANCE X-ray powder diffractometer ($\text{Cu K}\alpha$, 1.5418 \AA). Solid-state fluorescence analyzes were performed on an Edinburgh FL-FS90 TCSPC

fluorescence spectrometer. Variable-temperature magnetic susceptibility measurements were undertaken on a Quantum Design MPMS-XL7 SQUID magnetometer with an applied field of 1000 Oe from 1.8 to 300 K. Data were corrected for diamagnetic contribution calculated from Pascal's constants.

2.2. Synthesis

2.2.1. Synthesis of $[\text{Gd}(\text{HBIC})_3]_n$ (1**).** A reaction mixture of H_2BIC (0.0162 g, 0.1 mmol), $\text{Gd}(\text{NO}_3)_3 \cdot 6\text{H}_2\text{O}$ (0.0451 g, 0.1 mmol), $\text{Na}_2\text{C}_2\text{O}_4$ (0.0134 g, 0.1 mmol), CH_3CN (5 mL) and EtOH (5 mL) was stirred for 20 min, then transferred and sealed in a 20 mL Teflon-lined autoclave. The system was heated in an oven at 393 K for 72 h and cooled to room temperature at 5 K h^{-1} . The resulting colorless flaky crystals were collected, washed with ethanol and dried in air. Yield: ca. 71% (based on Gd). Anal. Calcd for $\text{C}_{24}\text{H}_{15}\text{N}_6\text{O}_6\text{Gd}$ (%): C, 44.99; H, 2.36; N, 13.12. Found (%): C, 45.21; H, 2.88; N, 12.92. IR (KBr)/ cm^{-1} : 3131(br, m), 1659(s), 1616(s), 1528(m), 1498(m), 1460(s), 1394(s), 1319(s), 1307(m), 1230(w), 1029(w), 989(w), 850(m), 821(m), 773(w), 741(s), 657(m), 592(m).

2.2.2. Synthesis of $[\text{Y}(\text{HBIC})_3]_n$ (2**).** An identical procedure with **1** was followed to prepare **2** except $\text{Gd}(\text{NO}_3)_3 \cdot 6\text{H}_2\text{O}$ was replaced by $\text{Y}(\text{NO}_3)_3 \cdot 6\text{H}_2\text{O}$ (0.0383 g, 0.1 mmol). Colorless flaky crystals of **2** were collected, yield: ca. 66% (based on Y). Anal. Calcd for $\text{C}_{24}\text{H}_{15}\text{N}_6\text{O}_6\text{Y}$ (%): C, 50.37; H, 2.64; N, 14.68. Found (%): C, 50.67; H, 2.20; N, 14.92. IR (KBr)/ cm^{-1} : 3137(br, m), 1647(s), 1599(s), 1524(m), 1490(m), 1443(s), 1389(s), 1322(s), 1301(m), 1219(w), 1013(w), 987(w), 824(m), 812(m), 769(w), 738(s), 628(m), 579(m).

2.3. X-ray crystallography

Single-crystal X-ray diffraction data for **1** and **2** were collected on a Bruker SMART APEXII CCD diffractometer equipped with graphite-monochromated $\text{Mo K}\alpha$ radiation ($\lambda = 0.71073 \text{ \AA}$) using ω and φ scan mode. All structures were solved by direct methods and refined with full-matrix least-squares based on F^2 using SHELXS-97 and SHELXL-97 [30, 31]. All nonhydrogen atoms were refined anisotropically. Hydrogens were placed in calculated positions. The detailed crystallographic data and structure refinement parameters of **1** and **2** are listed in table S1. Selected bond distances, angles, and hydrogen bonds are given in tables S2 and S3.

3. Results and discussion

3.1. Synthesis and characterization

1 and **2** in this study were prepared in modest to good yields by hydrothermal reactions. The samples used for all property determination were single crystals selected using a microscope. Additionally, to confirm the high purity of the as-synthesized **1**, crushed

crystalline samples were characterized by PXRD at room temperature, which is shown in Supplementary material. The pattern simulated from the single-crystal X-ray data of **1** is in agreement with the experimental one. Thus, the sample is proved as a single phase.

Overall, IR spectra of **1** and **2** are extremely similar, which further evidences that they are isomorphous. Spectra of **1** and **2** show characteristic bands at $\sim 1650\text{ cm}^{-1}$ and $\sim 1390\text{ cm}^{-1}$ (C=O, C=N stretching of HBIC[−]) and peaks at $\sim 3130\text{ cm}^{-1}$ attributed to $\nu(\text{N-H})$ in imidazole ring.

3.2. Structural description

The X-ray structural determination reveals that **1** and **2** are isostructural and crystallize in the monoclinic space group $P2_1/n$, featuring a 3-D supramolecular architecture constructed by 2-D wave-like networks through strong interlayer hydrogen-bonding interactions; thus, only the structure of **1** is described in detail. As shown in figure 1, each asymmetric unit consists of one crystallographically unique Gd(III) and three HBIC[−]. Gd(III) is a distorted bicapped triangle prism coordination geometry, coordinated by five carboxyl oxygens and three nitrogens from five HBIC[−]. The Gd–O distances are 2.332(7)–2.479(6) Å with mean of 2.407(6) Å and the average Gd–N bond distance is 2.543(7) Å. The average O–Gd–O bond angle is $105.5(2)^\circ$, similar to that of N–Gd–N [$105.6(3)^\circ$], but much larger than the mean O–Gd–N bond angle of $94.9(2)^\circ$ (table S2).

H₂BIC possesses strong coordination ability, coordinating with flexible and diverse coordination modes. To date, three types of coordination modes of H₂BIC have been reported (scheme 1(b)–(d)) [23–26], whereas in **1**, HBIC[−] serves as a chelating–bridging μ_2 -κN, O:κO coordination (scheme 1(a)) and a simple μ_1 -κN,O coordination (scheme 1(b)). As shown in figure 2, adjacent Gd(III) ions are linked by HBIC[−] with μ_2 -κN,O:κO mode to form an extended chain, and these extended infinite chains are further interweaved, generating a 2-D wave-like layered structure in the *ab* plane (figure 3(a)). Finally, a 3-D supramolecular architecture (figure 3(b)) is built by these 2-D layers *via* strong interlayer hydrogen-bonding interactions between oxygens and uncoordinated nitrogens from

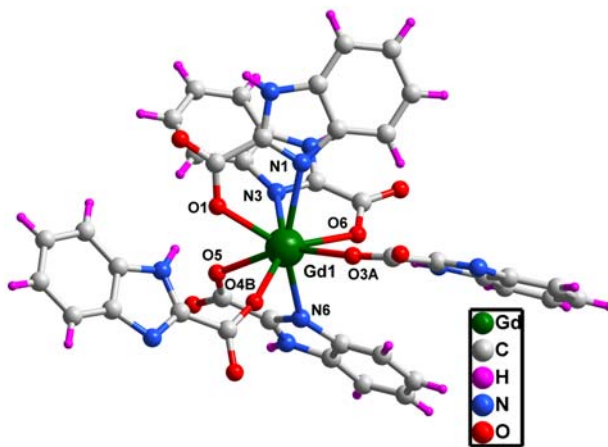


Figure 1. Coordination environment of Gd(III) in **1**; hydrogens are omitted for clarity. Symmetry codes: $A = 1/2 - x, 1/2 + y, 1/2 - z$; $B = -1/2 - x, 1/2 + y, 1/2 - z$.

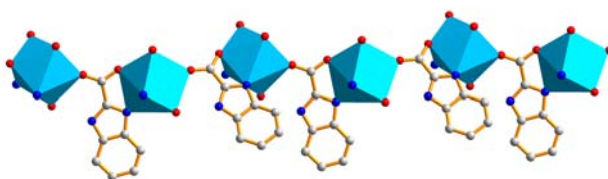


Figure 2. 1-D infinite chain structure in **1**; hydrogens are omitted for clarity.

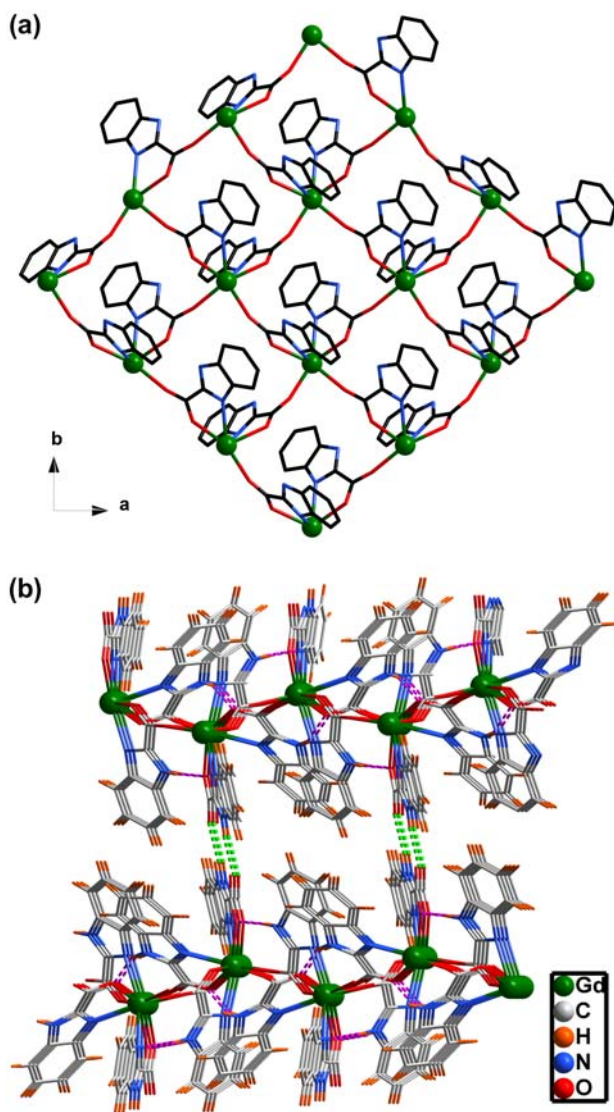


Figure 3. (a) 2-D wave-like network in **1**; hydrogens are omitted for clarity. (b) 3-D supramolecular architecture assembled *via* intralayer (pink-dashed lines) and interlayer (green-dashed lines) hydrogen bonds in **1** (see <http://dx.doi.org/10.1080/00206814.2013.775574> for color version).

HBIC[−] ligands [N4...O6^{#2} 2.729(10) Å, #2: $-x + 1/2, y - 1/2, -z + 1/2$] (table S3). Similar with other compounds with imidazole-carboxylic acid [32–34], the imidazole-carboxylic acid ligands form abundant hydrogen bonds as accepters or donors to consolidate the final 3-D framework.

3.3. Thermal analysis

Thermal gravity and differential thermal gravity analysis (TG-DTG) analyzes were performed between 30 and 800 °C at a heating rate of 10 °C min^{−1} in air. **1** and **2** are isomorphous, so only the thermogravimetric performance of **1** is described thoroughly. The TG-DTG graph of **1** (Supplementary material) shows clearly that the mass loss is implemented in only one step. From 322 to 515 °C, the weight loss of 71.89% corresponds to loss of HBIC[−] (Calcd 71.71%). At 600 °C, a final residue is stable, of 28.59%, identified as Gd₂O₃ (Calcd 28.29%). The relative DTG graph signifies the mass reduction happened in one thermal decomposition process, and the sharp peak at 383 °C indicates the fastest decomposition process.

In addition, the thermal stability analyzes of the two samples were also investigated by DSC with a heating rate of 10 °C min^{−1} from 30 to 800 °C (Supplementary material). The DSC curves of the two samples are similar, and each shows a broad exothermic peak, corresponding to the main framework collapse. For **1**, the peak temperature is 478 °C, which is 5 °C higher than **2** (473 °C), ascribed to the different radii of the metals.

3.4. Magnetic property of **1**

The temperature-dependent magnetic susceptibility measurements of **1** have been performed on crushed crystalline samples from 1.8 to 300 K at an external field of 1000 Oe with a Quantum Design MPMS-XL7 SQUID magnetometer. The experimental susceptibilities were corrected for Pascal's constants. Temperature dependencies of the magnetic susceptibilities as $\chi_m T$ and χ_m^{-1} versus T for **1** are given in figure 4. In the high-temperature region, the $\chi_m T$ value (300 K) is 8.28 cm³ K mol^{−1}, slightly larger than the theoretical value

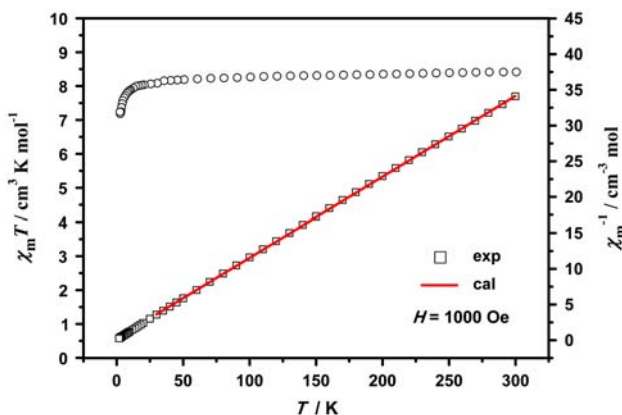


Figure 4. Temperature dependence of $\chi_m T$ and χ_m^{-1} value for **1** at 1000 Oe between 1.8 and 300 K.

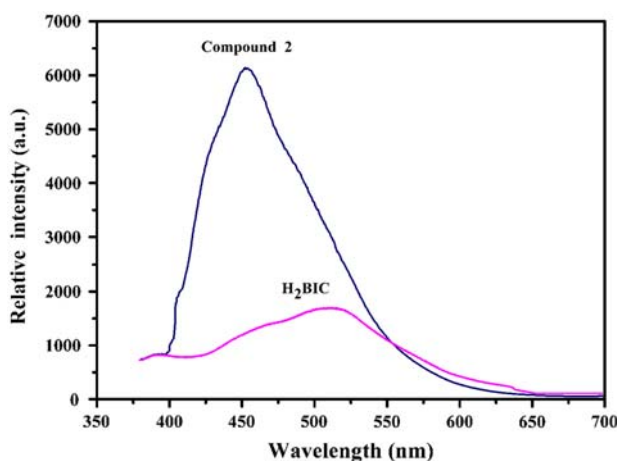


Figure 5. Room temperature emission spectra for H₂BIC and **2** ($\lambda_{\text{ex}} = 380$ nm) in the solid state.

of $7.88 \text{ cm}^3 \text{ K mol}^{-1}$ for one isolated Gd(III) ion with a $^8\text{S}_{7/2}$ ground state [35]. When the temperature decreases to ~ 9 K, the $\chi_m T$ value decreases smoothly and to $8.07 \text{ cm}^3 \text{ K mol}^{-1}$, upon further cooling, the $\chi_m T$ falls sharply, reaching a value of $7.16 \text{ cm}^3 \text{ K mol}^{-1}$ at 1.8 K. This indicates that there exist antiferromagnetic couplings between neighboring Gd(III) ions. The best linear fit according to the Curie–Weiss law [$\chi_m = C/(T - \theta)$] in the temperature range of 30–300 K yields $C = 8.85 \text{ cm}^3 \text{ K mol}^{-1}$ and Weiss constant $\theta = -2.37$ K. The negative Weiss constant and the decrease in $\chi_m T$ bear evidence of antiferromagnetic interaction between Gd(III) centers.

3.5. Fluorescence of **2**

Trivalent rare earth ions [e.g. Eu(III), Tb(III), Sm(III), Dy(III), and Y(III)] always display fascinating optical properties, and thus, the design of efficient rare earth compounds has become an important research goal, pursued by many groups [36–42]. Many rare earth compounds containing pyridine/imidazole carboxylate ligands have presented interesting luminescent behavior [32, 34, 43, 44]. As an effective chromophore, H₂BIC is used to construct luminescent materials containing rare earth ions. Figure 5 shows the emission spectra of free H₂BIC and **2** in the solid state at room temperature. Upon excitation at 380 nm, free H₂BIC shows one emission at 510 nm, while **2** exhibits strong blue luminescence with an emission at 453 nm. After adding Y(III) to H₂BIC, the fluorescence spectrum of the system changes in wavelength shift and the fluorescence intensity is significantly enhanced. Compared with the emission spectrum of H₂BIC, a blue shift of 57 nm in **2** arises from coordination of Y(III) with the ligand, which may be assigned to intraligand fluorescent emission. The result indicates that the fluorescence of this system belongs to Y(III) perturbed fluorescence of ligand or L*–L luminescence, suggesting that the compound is a promising candidate for luminescent materials.

4. Conclusion

Two new rare earth compounds incorporating H₂BIC have been hydrothermally synthesized and structurally characterized. **1** and **2** are isomorphous, both with 3-D supramolecu-

lar architectures constructed by 2-D wave-like networks *via* strong interlayer hydrogen bonds, which effectively enhance the thermal stability of the frameworks (stable up to $\sim 320^\circ\text{C}$). Variable-temperature magnetic study for **1** suggests that the magnetic interactions between Gd(III) ions are mainly antiferromagnetic coupling. Luminescence demonstrates that **2** exhibits strong blue emission with blue shift, which may be assigned to intraligand emission.

Supplementary material

Crystallographic details, selected bond lengths (\AA) and angles ($^\circ$) as well as hydrogen-bonding interactions for **1** and **2** are available. CCDC-895931 (for **1**) and CCDC-874300 (for **2**) contain the supplementary crystallographic data for this article. These data can be obtained free of charge from the Cambridge Crystallographic Data Center *via* www.ccdc.cam.ac.uk/data_request/cif.

Acknowledgments

We gratefully acknowledge the financial support from the National Natural Science Foundation of China (Grant nos. 21073142, 21173168, 21273171 and 21127004), the Natural Science Foundation of the Department of Education of Shaanxi Province (Grant nos. 11JS110, 2010JK882, 2010JQ2007, 08JK459 and 11JK0578) and the Natural Science Foundation of Shangluo University (Grant no. 12SKY012).

References

- [1] G.F. Wang, Q. Peng, Y.D. Li. *Acc. Chem. Res.*, **44**, 322 (2011).
- [2] J. Fan, S.W. Boettcher, C.K. Tsung, Q.H. Shi, M. Schierhorn, G.D. Stucky. *Chem. Mater.*, **20**, 909 (2008).
- [3] S. Das, K.C. Mandal. *Mater. Lett.*, **66**, 46 (2012).
- [4] D. Liu, Z.G. Wang. *Polymer*, **49**, 4960 (2008).
- [5] S.L. Qiu, G.S. Zhu. *Coord. Chem. Rev.*, **253**, 2891 (2009).
- [6] S. Chandra, F.L. Deepak, J.B. Gruber, D.K. Sardar. *J. Phys. Chem. C*, **114**, 874 (2010).
- [7] X.J. Zhao, G.S. Zhu, Q.R. Fang, Y. Wang, F.X. Sun, S.L. Qiu. *Cryst. Growth Des.*, **9**, 737 (2009).
- [8] Z. Shen, G. Zhang, H. Zhou, P. Sun, B. Li, D. Ding, T. Chen. *Adv. Mater.*, **20**, 984 (2008).
- [9] Y.G. Huang, B.L. Wu, D.Q. Yuan, Y.Q. Xu, F.L. Jiang, M.C. Hong. *Inorg. Chem.*, **46**, 1171 (2007).
- [10] J.P. Leonard, P. Jensen, T. McCabe, J.E. O'Brien, R.D. Peacock, P.E. Kruger, T. Gunnlaugsson. *J. Am. Chem. Soc.*, **129**, 10986 (2007).
- [11] B. Moulton, M.J. Zaworotko. *Chem. Rev.*, **101**, 1629 (2001).
- [12] E.C. Yang, H.K. Zhao, B. Ding, X.G. Wang, X.J. Zhao. *Cryst. Growth Des.*, **7**, 2009 (2007).
- [13] Q. Sun, Q. Yue, J.Y. Zhang, L. Wang, X. Li, E.Q. Gao. *Cryst. Growth Des.*, **9**, 2310 (2009).
- [14] E. Shyu, R.M. Supkowski, R.L. LaDuca. *Cryst. Growth Des.*, **9**, 2481 (2009).
- [15] M. Xue, G.S. Zhu, Y.X. Li, X.J. Zhao, Z. Jin, E. Kang, S.L. Qiu. *Cryst. Growth Des.*, **8**, 2478 (2008).
- [16] J.Q. Chen, Y.P. Cai, H.C. Fang, Z.Y. Zhou, X.L. Zhan, G. Zhao, Z. Zhang. *Cryst. Growth Des.*, **9**, 1605 (2009).
- [17] C.H. Li, K.L. Huang, Y.N. Chi, X. Liu, Z.G. Han, L. Shen, C.W. Hu. *Inorg. Chem.*, **48**, 2010 (2009).
- [18] Z.W. Wang, C.C. Ji, J. Li, Z.J. Guo, Y.Z. Li, H.G. Zheng. *Cryst. Growth Des.*, **9**, 475 (2009).
- [19] N.E. Dean, R.D. Hancock, C.L. Cahill, M. Frisch. *Inorg. Chem.*, **47**, 2000 (2008).
- [20] N.R. Kelly, S. Goetz, S.R. Batten, P.E. Kruger. *CrystEngComm*, **10**, 1018 (2008).
- [21] A. de Bettencourt-Dias, S. Viswanathan. *Dalton Trans.*, 4093 (2006).
- [22] S. Viswanathan, A. de Bettencourt-Dias. *Inorg. Chem.*, **45**, 10138 (2006).
- [23] S.R. Zheng, S.L. Cai, J. Fan, T.T. Xiao, W.G. Zhang. *Inorg. Chem. Commun.*, **14**, 818 (2011).
- [24] J. Fan, S.L. Cai, S.R. Zheng, W.G. Zhang. *Acta Crystallogr.*, **C67**, m346 (2011).

- [25] F. Sączewski, E. Dziemidowicz-Borys, P.J. Bednarski, R. Grünert, M. Gdaniec, P. Tabin. *J. Inorg. Biochem.*, **100**, 1389 (2006).
- [26] L.L. Di, Y. Wang, G.W. Lin, T. Lu. *Acta Crystallogr.*, **E66**, m610 (2010).
- [27] G.X. Liu, K. Zhu, H.M. Xu, S. Nishihara, R.Y. Huang, X.M. Ren. *CrystEngComm*, **12**, 1175 (2010).
- [28] D.S. Li, Y.P. Wu, P. Zhang, M. Du, J. Zhao, C.P. Li. *Cryst. Growth Des.*, **10**, 2037 (2010).
- [29] I. Wiedermannová, J. Slouka, K. Lemr. *Heterocycl. Commun.*, **8**, 479 (2002).
- [30] G.M. Sheldrick. *SHELXS-97 Program for X-ray Crystal Structure Determination*, University of Göttingen, Göttingen, Germany (1997).
- [31] G.M. Sheldrick. *SHELXL-97, Program for X-ray Crystal Structure Refinement*, University of Göttingen, Göttingen, Germany (1997).
- [32] L.Z. Chen, F.M. Wang, H. Shu. *J. Coord. Chem.*, **65**, 439 (2012).
- [33] N. Chen, Y. Zhang, Z.L. Yang, G. Li. *J. Coord. Chem.*, **65**, 1221 (2012).
- [34] M.W. Guo, N. Chen, Y.C. Gao, H.J. Lu, G. Li. *J. Coord. Chem.*, **65**, 1724 (2012).
- [35] C. Benelli, D. Gatteschi. *Chem. Rev.*, **102**, 2369 (2002).
- [36] J.C.G. Bünzli, S. Comby, A.S. Chauvin, C.D.B. Vandevyver. *J. Rare Earths*, **25**, 257 (2007).
- [37] E.G. Moore, A.P.S. Samuel, K.N. Raymond. *Acc. Chem. Res.*, **42**, 542 (2009).
- [38] K. Kuriki, Y. Koike, Y. Okamoto. *Chem. Rev.*, **102**, 2347 (2002).
- [39] K. Binnemans, C. Gorller-Walrand. *Chem. Rev.*, **102**, 2303 (2002).
- [40] X.Y. Zhang, Y. Li, D.D. Qi, J.Z. Jiang, X.Z. Yan, Y.Z. Bian. *J. Phys. Chem. B*, **114**, 13143 (2010).
- [41] K. Yoshino, S.B. Lee, T. Sonoda, H. Kawagishi, R. Hidayat, K. Nakayama, M. Ozaki, K. Ban, K. Nishizawa, K. Ohta, H. Shirai. *J. Appl. Phys.*, **88**, 7137 (2000).
- [42] L. Shen, J. Yang, Y.S. Ma, X.Y. Tang, G.W. Yang, Q.Y. Li, F. Zhou, Z.F. Miao, X.W. Fei, J.W. Huang. *J. Coord. Chem.*, **64**, 431 (2011).
- [43] L. Wang, L. Ni. *J. Coord. Chem.*, **65**, 1475 (2012).
- [44] S. Sharif, O. Sahin, I.U. Khan, O. Büyükgüngör. *J. Coord. Chem.*, **65**, 1892 (2012).